Theoretical Mechanistic Study on the Radical−Molecule Reaction of CH_2OH with NO_2

Jia-xu Zhang, Ze-sheng Li,* Jing-yao Liu, and Chia-Chung Sun

Institute of Theoretical Chemistry, State Key Laboratory of Theoretical and Computational Chemistry, Jilin University, Changchun 130023, P. R. China

Received: September 28, 2005; In Final Form: November 27, 2005

The complex singlet potential energy surface for the reaction of CH_2OH with NO_2, including 14 minimum isomers and 28 transition states, is explored theoretically at the B3LYP/6-311G(d,p) and Gaussian-3 (single-point) levels. The initial association between CH_2OH and NO_2 is found to be the carbon-to-nitrogen approach forming an adduct $HOCH_2NO_2$ (**1**) with no barrier, followed by C−N bond rupture along with a concerted H-shift leading to product $\mathbf{P_1}$ (CH_2O + *trans*-HONO), which is the most abundant. Much less competitively, **1** can undergo the C−O bond formation along with C−N bond rupture to isomer $HOCH_2ONO$ (**2**), which will take subsequent *cis*−*trans* conversion and dissociation to $\mathbf{P_2}$ (HOCHO + HNO), $\mathbf{P_3}$ (CH_2O + HNO_2), and $\mathbf{P_4}$ (CH_2O + *cis*-HONO) with comparable yields. The obtained species CH_2O in primary product $\mathbf{P_1}$ is in good agreement with kinetic detection in experiment. Because the intermediate and transition state involved in the most favorable pathway all lie blow the reactants, the CH_2OH + NO_2 reaction is expected to be rapid, as is confirmed by experiment. These calculations indicate that the title reaction proceeds mostly through singlet pathways; less go through triplet pathways. In addition, a mechanistic comparison is made with the reactions CH_3 + NO_2 and CH_3O + NO_2. The present results can lead us to deeply understand the mechanism of the title reaction and may be helpful for understanding NO_2-combustion chemistry.

1. Introduction

Radical−radical cross-combination reactions constitute an integral part of the overall mechanisms of oxidation and pyrolysis of hydrocarbons.[1,2] Hydroxyalkyl radicals are important intermediates in the oxidation processes that occur in both combustion[3] and atmospheric chemistry.[4,5] Despite this, there have been very few studies involving this class of intermediates; this is in contrast to the many studies involving the isomeric species, the alkoxy radicals.[6−8] The simplest member of the hydroxyalkyl class of intermediates is the hydroxymethyl radical, CH_2OH. Previous studies involving this species have concentrated on the mutual reaction and its reaction with O_2.[9−13] On the other hand, it is known that nitrogen oxides (NO_x $x = 1, 2$) are among the major atmospheric pollutants released by combustion process. To minimize the harmful effects before their release in the atmosphere, one effective way is to chemically reduce them by the reburning of combustion products.[14−19] The reaction of hydroxymethyl radical with NO_2 can be expected to be important during the oxidation of hydroxyalkyl compounds at low temperatures, because traces of nitrogen oxides are also often present.[20] Hence, reliable information on the kinetics of this hydroxymethyl reaction is of importance for the modeling of NO_x-combustion processes.

In the last two decades, the studies of the reactions of halocarbene with NO_x have been the important topic due to the role of inhibition.[21−24] However, the number of the substituted methyl radical reactions with NO_2 subjected to direct kinetic studies is few. Up to now, Nesbitt et al.[25] have investigated the reaction of hydroxymethyl radical (CH_2OH) with NO_2 at low pressures (∼1 Torr He) using a discharge-flow system combined with a mass spectrometer and obtained a bimolecular rate coefficient of $(8.3 \pm 4.1) \times 10^{-12}$ cm^3 molecule^{-1} s^{-1} at room temperature. The observed major product by them was CH_2O. Pagsberg et al.[26] have studied the same reaction at room temperature and atmospheric pressure obtaining a rate coefficient of $(2.3 \pm 0.4) \times 10^{-11}$ cm^3 molecule^{-1} s^{-1} using pulse radiolysis to generate radicals and UV absoption to measure the kinetics. The measured rate constant values indicate that the title reaction is very rapid and may be very important in the NO_x-combustion chemistry. However, the available information on product channels, product distributions, and reaction mechanism were not further provided though this information may be important in the NO_2-involved sequential chain processes. To our best knowledge, no report is found about the theoretical study on the title reaction. In addition, recently, we have built up the potential energy surface of the analogous CH_3 + NO_2 reaction.[27] Now, the sequential question is whether the mechanism of the title reaction CH_2OH + NO_2 is similar to the CH_3 + NO_2 reaction?

In view of the potential importance and the rather limited information, we carry out a detailed theoretical study on the potential energy surface (PES) of the CH_2OH + NO_2 reaction to (1) provide the elaborated isomerization and dissociation channels on the $HOCH_2NO_2$ PES, (2) investigate the products of this reaction to assist in further experimental identification, and (3) make comparisons between the CH_2X (X = H, OH) reactions with NO_2 and between CH_2OH + NO_2 and CH_3O + NO_2 reactions to give a deep insight into the mechanism of the hydroxymethyl-NO_2-combustion reaction.

2. Computational Methods

All calculations are carried out using the GAUSSIAN98 program.[28] All structures of the stationary points including reactants, minimum isomers, transition states, and products are calculated using hybrid density functional B3LYP method[29] (the

* Corresponding author. Fax: +86-431-8945942. E-mail: Zeshengli@mail.jlu.edu.cn.

10.1021/jp055515x CCC: $33.50
Published on Web 02/07/2006

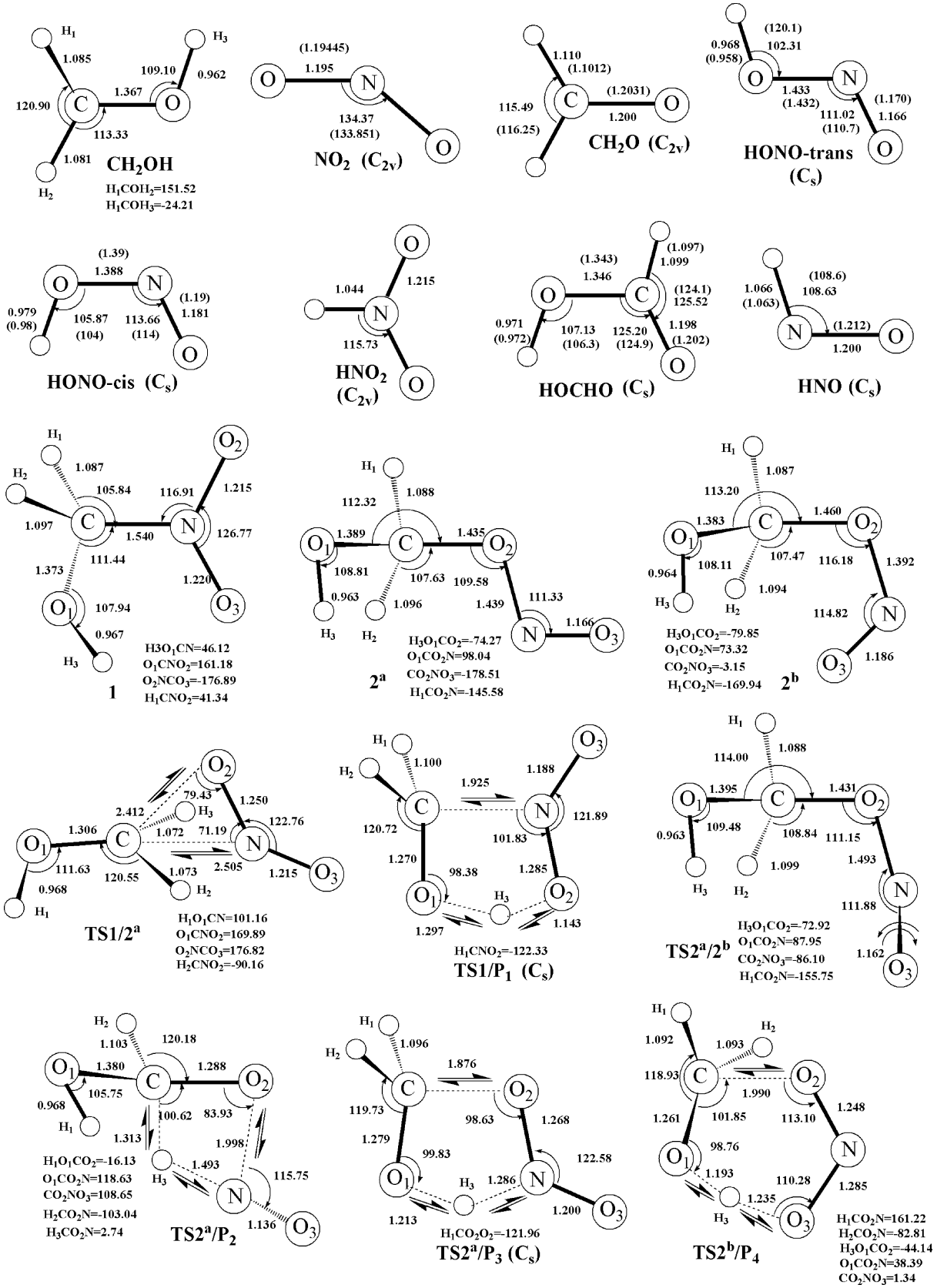

Figure 1. B3LYP/6-311G(d,p) optimized geometries of reactants, some important products, isomers and transition states for $CH_2OH + NO_2$ reaction. Bond distances are in angstroms, and angles are in degrees. The values in parentheses are the experimental data (ref 34 for NO_2 and CH_2O; ref 35 for *trans*-HONO, *cis*-HONO, HOCHO, and HNO). In the transition states the direction of the imaginary frequency is indicated by "⇌".

Becke's three parameter hybrid functional with the nonlocal correlation functional of Lee−Yang−Parr) with 6-311G(d,p) basis set.[30−32] The spin-unrestricted B3LYP were applied to doublet of fragment molecules. The stationary nature of structures is confirmed by harmonic vibrational frequency calculations (i.e., equilibrium species possess all real frequen-

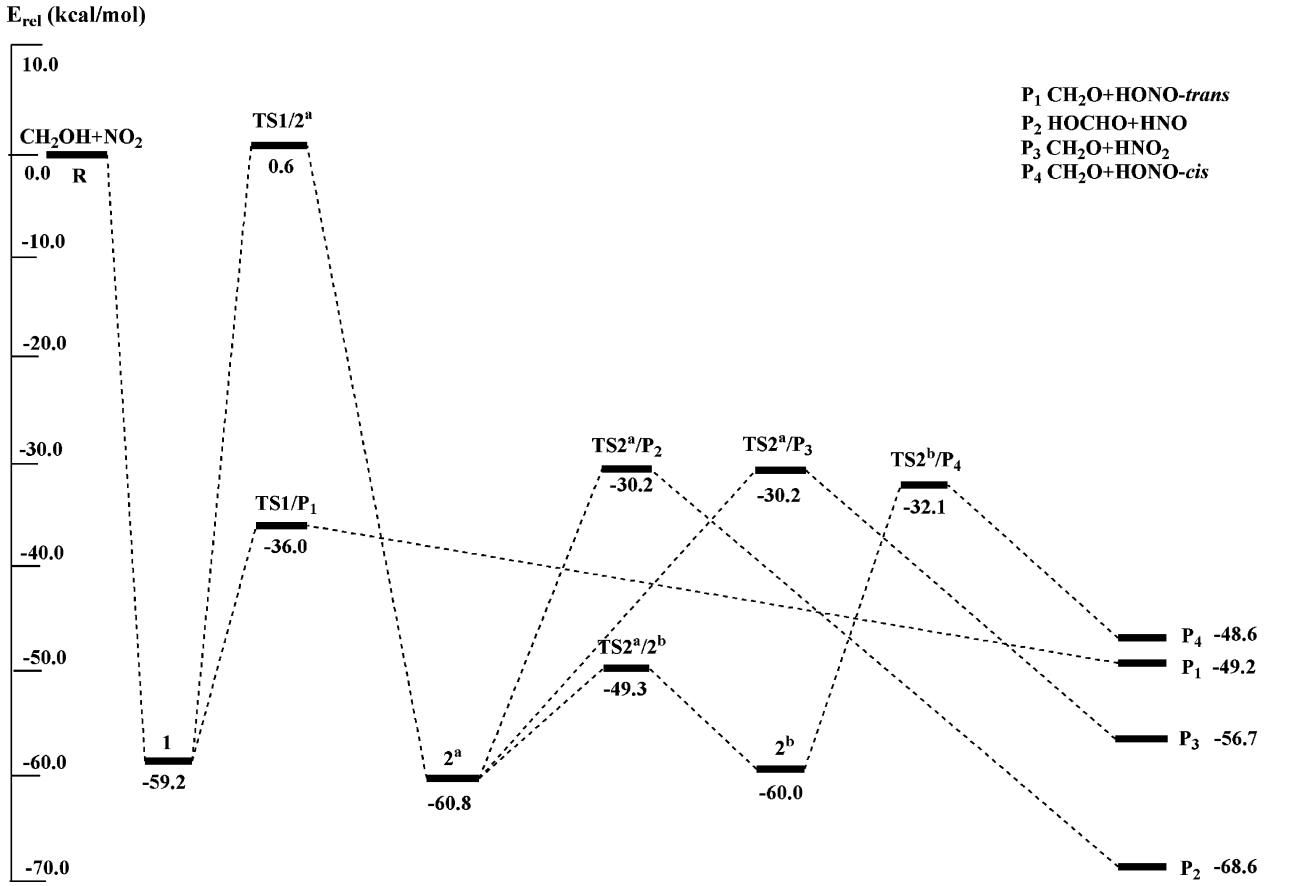

Figure 2. Schematic singlet potential energy surface of the most relevant reaction channels for the $CH_2OH + NO_2$ reaction at the G3//B3LYP/6-311G(d,p) + ZPE level. E_{rel} are the relative energies (kcal/mol).

cies), whereas transition states possess one and only one imaginary frequency. The zero-point energy (ZPE) corrections are obtained at the same level of theory. To yield more accurate energetic information, higher level single-point energy calculations are performed at the multilevel techniques based on additive energy corrections (e.g., G3[33]) level by using the B3LYP/6-311G(d,p) optimized geometries. To confirm that the transition states connect designated intermediates, intrinsic reaction coordinate (IRC) calculation is carried out at the B3LYP/6-311G(d,p) level. Unless otherwise specified, the G3 single-point energies with zero-point energy (ZPE) corrections (simplified as G3//B3LYP) are used in the following discussions.

3. Results and Discussion

The optimized structures of the important stationary points with the corresponding experimental data[34,35] are depicted in Figure 1, whereas the unfavorable ones are presented in Figure S1 (Supporting Information).[36] Table 1 displays the relative energies including ZPE corrections of the stationary points with available experimental data[35,37] for comparison. For our discussion easier, the energy of reactants **R** is set to be zero for reference. As shown by Table 1, our calculated relative energies and the experimentally determined reaction heats of the products are very close to each other with the discrepancy less than 3 kcal/mol. Moreover, for the reactants CH_2OH and NO_2, the calculated heats of formation are in good agreement with experimental values with the largest deviation of 1.49 kcal/mol. The harmonic vibrational frequencies of the important species including available experimental data[37] are listed in Table S1 (Supporting Information).[36] Note that the calculated geometries and frequencies agree very well with experimental results within 7% at the B3LYP/6-311G(d,p) level. To clarify the reaction mechanism, the most relevant pathways of the singlet PES for $CH_2OH + NO_2$ reaction at the G3//B3LYP level are plotted in Figure 2. The unfavorable reaction channels are depicted in Figure 3.

TABLE 1: Calculated Heats of Formation for Reactants ($\Delta H_f^\circ{}_{298}$, kcal/mol) and Relative Energies (E_{rel}, kcal/mol) (with Inclusion of the B3LYP/6-311G(d,p) Zero-Point Energy (ZPE) Corrections) of Reactants, Some Important Products, Isomers, and Transition States at the G3//B3LYP/6-311G(d,p) Level and Available Experimental Values

species	E_{rel}	$\Delta H_f^\circ{}_{298}$	expt
CH_2OH		−3.5	−3.1[a]
NO_2		9.4	7.91[a]
R, $CH_2OH + NO_2$	0.0		
P1, CH_2O + *trans*-HONO	−49.2		−49.8[b]
P2, HOCHO + HNO	−68.6		−71.6[b]
P3, $CH_2O + HNO_2$	−56.7		
P4, CH_2O + *cis*-HONO	−48.6		
1	−59.2 (−54.8)		
2a	−60.8 (−56.8)		
2b	−60.0 (−57.2)		
TS1/2a	0.6 (2.7)		
TS1/P1	−36.0 (−32.3)		
TS2a/2b	−49.3 (−45.5)		
TS2a/P2	−30.2 (−27.3)		
TS2a/P3	−30.2 (−26.4)		
TS2b/P4	−32.1 (−28.3)		

[a] Experimental heats of formation from ref 37. [b] Experimental reaction heats from refs 35 and 37. The values in the parentheses including BSSE correction.

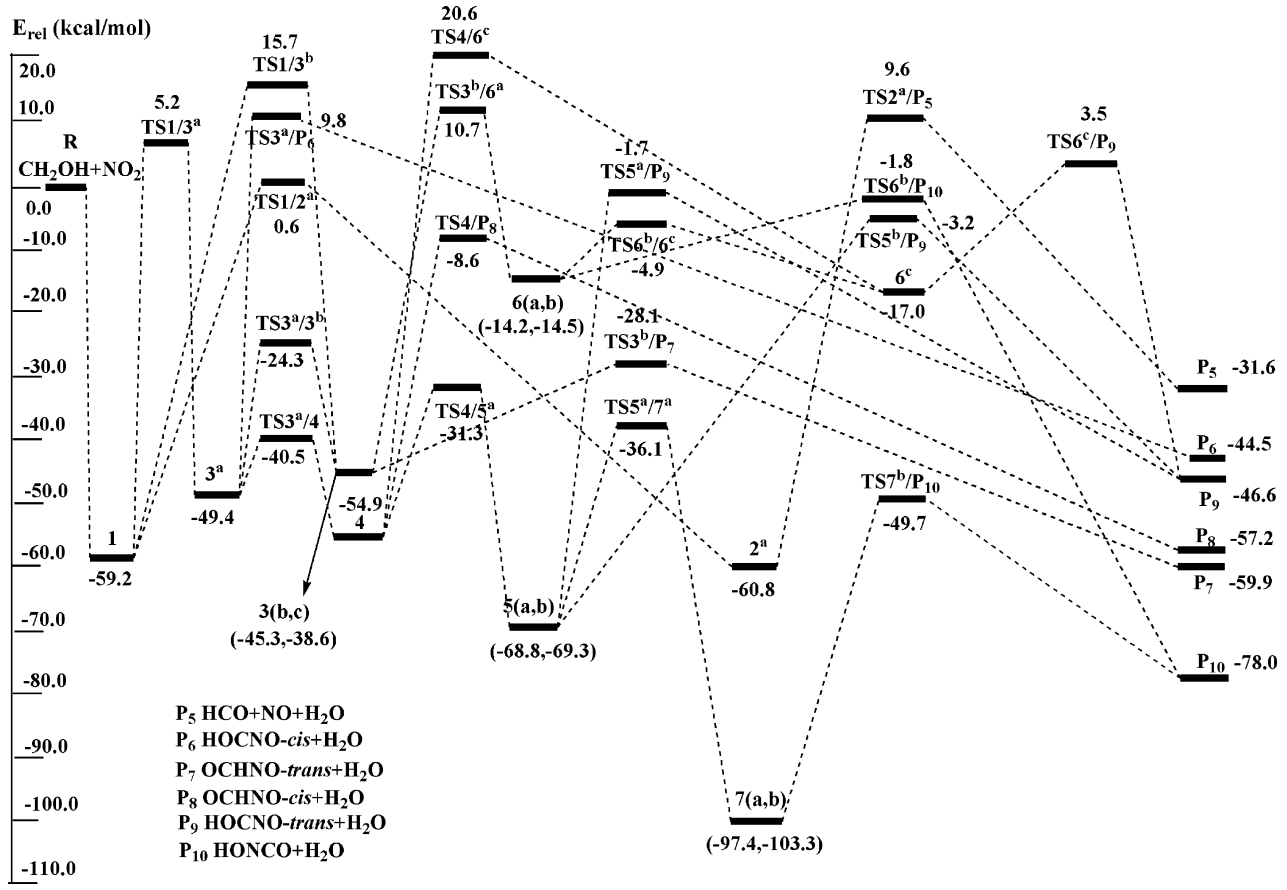

Figure 3. Schematic singlet potential energy surface of unfavorable reaction channels for the $CH_2OH + NO_2$ reaction at the G3//B3LYP/6-311G-(d,p) + ZPE level. E_{rel} are the relative energies (kcal/mol).

3.1. Initial Association. Both singlet and triplet CH_2OHNO_2 potential energy surfaces (PES) may be obtained for the radical−molecule reaction of CH_2OH and NO_2. On the singlet PES, the carbon-to-nitrogen approach is rather attractive to form isomer **1** ($HOCH_2NO_2$) without any encounter barrier. The association is expected to be fast and to play a significant role in the reaction kinetics. We are unable to locate the transition state for the carbon-to-oxygen attack forming isomer **2** ($HOCH_2ONO$) at the B3LYP/6-311G(d,p) level. Yet, we expect that considerable barrier is needed to activate the short N═O double bond (1.195 Å in NO_2) to form the long N−O single bonds (1.439 Å in $\mathbf{2^a}$, 1.392 Å in $\mathbf{2^b}$). On the triplet PES, the carbon-to-nitrogen attacking isomer $^3\mathbf{1}$ ($HOCH_2NO_2$) is located, whereas it lies 8.0 kcal/mol above the reactants **R**. Therefore, the formation of $^3\mathbf{1}$ is thermodynamically almost prohibited. Furthermore, the carbon-to-oxygen attack can lead to the triplet isomer $^3\mathbf{2^a}$ (*trans*-$HOCH_2ONO$) (−3.9 kcal/mol) via the transition state $^3\mathbf{TSR/2^a}$ with a high barrier of 13.5 kcal/mol. In view of the much higher entrance barriers, the triplet pathways may contribute less to the $CH_2OH + NO_2$ reaction compared with the singlet pathways and thus will not be further discussed. As a result, this reaction is most likely initiated by the carbon-to-nitrogen approach on the singlet PES, just in accordance with the dominant spin density on the nitrogen (0.449) rather than oxygen (0.276) atom in NO_2 molecule. In the following discussions, we mainly discuss the formation pathways of various products proceeded via isomer **1** $HOCH_2NO_2$.

3.2. Isomerization and Dissociation Pathways. With the very large exothermicity released from the reactants **R**, the initial formed isomer **1** ($HOCH_2NO_2$) can take various isomerization followed by final decomposition. For clarity, we first show the former feasible pathways from isomer **1** (in Figure 2):

Path 1: $HOCH_2NO_2$ (**1**) → $\mathbf{P_1}$ (CH_2O + *trans*-HONO)

Path 2: $HOCH_2NO_2$ (**1**) → *trans*-$HOCH_2ONO$ ($\mathbf{2^a}$) → $\mathbf{P_2}$ (HOCHO + HNO)

Path 3: $HOCH_2NO_2$ (**1**) → *trans*-$HOCH_2ONO$ ($\mathbf{2^a}$) → $\mathbf{P_3}$ ($CH_2O + HNO_2$)

Path 4: $HOCH_2NO_2$ (**1**) → *trans*-$HOCH_2ONO$ ($\mathbf{2^a}$) → *cis*-$HOCH_2ONO$ ($\mathbf{2^b}$) → $\mathbf{P_4}$ (CH_2O + *cis*-HONO)

The direct C−N bond rupture along with a concert H-shift of isomer **1** can lead to product $\mathbf{P_1}$ (CH_2O + *trans*-HONO) as in path 1. Alternatively, **1** can isomerize to isomer $\mathbf{2^a}$ via the C−O2 bond formation along with C−N bond rupture. The isomeric pair $\mathbf{2^a}$ and $\mathbf{2^b}$ can be converted to each other via a N−O single bond rotation with the barriers of 11.5 ($\mathbf{2^a} \rightarrow \mathbf{2^b}$) and 10.7 ($\mathbf{2^b} \rightarrow \mathbf{2^a}$) kcal/mol, respectively. Subsequently, $\mathbf{2^a}$ can take the O2−N bond cleavage associated with a concert H-shift to give $\mathbf{P_2}$ (HOCHO + HNO) as in path 2 or dissociate to $\mathbf{P_3}$ ($CH_2O + HNO_2$) via the C−O2 bond rupture along with the concert H-shift as in path 3, whereas $\mathbf{2^b}$ may undergo a concert H-shift accompanied by O1−N bond fission to form $\mathbf{P_4}$ (CH_2O + *cis*-HONO) as in path 4.

As shown in Figure 2, in paths 1−4, all the isomers and transition states are almost lower than the reactants **R** in energy

except for **TS1/2[a]** with a much smaller positive value of 0.6 kcal/mol. As a result, paths 1−4 are favorable for the total reaction.

Now, we turn our attention to the unfavorable pathways shown in Figure 3. We can find that a 1,3-H-shift from C-atom to O2-atom associated with a concerted twist of isomer **1** can form isomer **3[a]** (*trans*-HOCHN(O)OH). It should be pointed out that the process **1** → **3[a]** is kinetically less feasible at normal temperatures due to the high-energy transition state **TS1/3[a]** above the reactants **R**. However, because the **1** → **3[a]** conversion barrier is just 5.2 kcal/mol above the reactants, the conversion may become feasible at high temperatures. Once such a high-energy transition state **TS1/3[a]** is surmounted, subsequently several important reaction pathways lie below the reactants. First, isomer **3[a]** can take cis−trans isomerization to isomer **3[b]** (*cis*-HOCHN(O)OH) followed by dissociation to product **P7** (*trans*-OCHNO + H_2O). Second, the 1,4-H-shift along with a concerted twist of isomer **3[a]** can lead to isomer **4** (OCHN(OH)-OH) followed by side-H_2O extrusion to product **P8** (*cis*-OCHNO + H_2O). In addition, isomer **4** can also undergo simultaneous 1,2-migration of the OH group and 1,4-H-shift to isomer **5[a]** (HO(HO)CHNO), which will easily interconvert to each other with its isomeric species **5[b]**. Then, both **5[a]** and **5[b]** can split to product **P9** (*trans*-HOCNO + H_2O) via side-H_2O elimination. Alternatively, isomer **5[a]** may continuously isomerize to isomer **7[a]** (*cis*-HO(O)CNHOH), and then to **7[b]** (*trans*-HO(O)CNHOH) followed by its dissociation to form product **P10** (HONCO + H_2O). These processes can simply be summarized as

Path 5: $HOCH_2NO_2$ (**1**) → *trans*-HOCHN(O)OH (**3[a]**) → *cis*-HOCHN(O)OH (**3[b]**) → **P7** (*trans*-OCHNO + H_2O)

Path 6: $HOCH_2NO_2$ (**1**) → *trans*-HOCHN(O)OH (**3[a]**) → OCHN(OH)OH (**4**) → **P8** (*cis*-OCHNO + H_2O)

Path 7: $HOCH_2NO_2$ (**1**) → *trans*-HOCHN(O)OH (**3[a]**) → HO(HO)CHNO (**5[a]**, **5[b]**) → **P9** (*trans*-HOCNO + H_2O)

Path 8: $HOCH_2NO_2$ (**1**) → *trans*-HOCHN(O)OH (**3[a]**) → HO(HO)CHNO (**5[a]**) → *cis*-HO(O)CNHOH (**7[a]**) → *trans*-HO(O)CNHOH (**7[b]**) → **P10** (HONCO + H_2O)

Because the available energy of 5.2 kcal/mol is generally required to drive these processes to proceed, the above four pathways leading to products **P7** (*trans*-OCHNO + H_2O), **P8** (*cis*-OCHNO + H_2O), **P9** (*trans*-HOCNO + H_2O), and **P10** (HONCO + H_2O) may be important in high-temperature processes. However, all of them are much less competitive than the favorable paths 1−4 leading to products **P1** (CH_2O + *trans*-HONO), **P2** (HOCHO + HNO), **P3** (CH_2O + HNO_2), and **P4** (CH_2O + *cis*-HONO), respectively.

On the other hand, as can be seen from Figure 3, the other isomerization and dissociation channels **1** → **3[b]**, **2[a]** → **P5** (HCO + NO + H_2O), **3[a]** → **P6** (*cis*-HOCNO + H_2O), **3[b]** → **6** (**a, b, c**) → **P9**, **P10**, and **4** → **6[c]** → **P9** all involve the high-energy transition states that lie significantly above the reactants **R** and much higher than the rate-determining transition states in paths 1−8. Therefore, all of them are kinetically unfeasible and cannot compete with paths 1−8. For simplicity, the detailed discussions will not be given here.

3.3. Reaction Mechanism and Experimental Implications. From the above analysis, it is clear that the CH_2OH radical can barrierlessly associate with NO_2 at the middle-N site to form the low-lying isomer **1** ($HOCH_2NO_2$). Although there are various isomerization and dissociation channels starting from isomer **1**, only pathways 1−4 are most probable. Among paths 1−4, the most competitive pathway should be path 1 because the rate-determining transition state **TS1/P1** (−36.0 kcal/mol) in path 1 lies much lower than **TS1/2[a]** (0.6 kcal/mol) in paths 2−4. Moreover, path 1 is the simplest pathway just associated with the direct dissociation, whereas paths 2−4 need to proceed by one lowing-lying and kinetically stable (reside in a deep potential well) species **2** (**2[a]**, **2[b]**). With respect to paths 2−4, they may compete intensively with each other because the overall barriers from the common intermediate **2[a]** to the final dissociation products are very close to each other with deviation less than 1.9 kcal/mol. In addition, the rate-determining transition state **TS1/3[a]** in paths 5−8 is only 5.2 kcal/mol higher than the reactants **R** in energy. So these four pathways may be of significance at high temperatures. As a result, reflected in the final product distributions, we predict that (1) product **P1** (CH_2O + *trans*-HONO) is the most favorable product; (2) **P2** (HOCHO + HNO), **P3** (CH_2O + HNO_2), and **P4** (CH_2O + *cis*-HONO) are the much less competitive products with a comparable yield; and (3) formation of products **P7** (*trans*-OCHNO + H_2O), **P8** (*cis*-OCHNO + H_2O), **P9** (*trans*-HOCNO + H_2O), and **P10** (HONCO + H_2O) may become possible only at high temperatures. Our results are in good agreement with the kinetic studies by Nesbitt et al.,[25] in which the observed major product is CH_2O that can be found as one species of the most feasible product CH_2O + *trans*-HONO in our calculations, whereas further kinetic investigations are still required for the unobserved species *trans*-HONO. Both Pagsberg et al.[26] and Nesbitt et al.[25] suggested that formation of an initial adduct that can dissociate to products after isomerization may dominate in the reaction of CH_2OH with NO_2. The suggested adduct has indeed been identified in our calculations (denoted as isomer **1**, $HOCH_2NO_2$), and on the basis of our present results, we find that this reaction proceeds through a multistep process of association and dissociation as described by path 1: **R** (CH_2OH + NO_2) → $HOCH_2NO_2$ (**1**) → **P1** (CH_2O + *trans*-HONO). Because the intermediate and transition state involved in this most feasible pathway (path 1) all lie below the reactants **R**, the CH_2OH + NO_2 reaction is expected to be fast at normal temperatures, as is confirmed by experiments.[25,26] Thus, the reaction between CH_2OH and NO_2 may play an important role in atmospheric and combustion chemistry and may be considered as an significant process, referred to as "reburning".[16−19]

Moreover, to further testify the reaction mechanism obtained at the G3//B3LYP level, the basis set superposition error (BSSE) correction for the critical species of the main channels is estimated using the counterpoise method. As shown by Table 1, When BSSE is considered, the relative energies increase about 3.5 kcal/mol in general. Additional BSSE correction can decrease the thermodynamic stability of the species relative to the reactants **R**. It is easily found from Table 1 that the features of PES with BSSE-correction are generally consistent with that without BSSE correction. (1) Path 1 should be the most favorable pathway. (2) Paths 2−4 may still compete intensively each other. However, all of them are much less feasible than path 1 and have less contribution to the total reaction. Thus, it is seen that in quality the reaction mechanisms as well as the possible products for the CH_2OH + NO_2 reaction are very similar with or without BSSE correction; we expect that the present G3//B3LYP results could be reliable for the title reaction.

Previously, a detailed theoretical investigation on the potential energy surface for CH_2OH reaction with NO_2 had been carried

out by Shields et al.[38] By comparing the theoretical results, we note the following: (1) The formation of the adducts $HOCH_2NO_2$ and $HOCH_2ONO$ predicted by Shields et al. is indeed identified in our calculations (denoted as isomers $HOCH_2NO_2$ (**1**) and $HOCH_2ONO$ (**2**)). Moreover, our calculations indicate that both of them can further dissociate to give various fragments. (2) The predicted products $CH_2O + HNO_2$ and CH_2O + HONO of reaction CH_2OH with NO_2 by Shields et al. are also located in our studies as the major product $\mathbf{P_1}$ (CH_2O + *trans*-HONO) and minor products $\mathbf{P_3}$ ($CH_2O + HNO_2$) and $\mathbf{P_4}$ (CH_2O + *cis*-HONO). (3) Our results agree with Shields et al.'s studies that all the four reaction pathways leading to $HOCH_2NO_2$, $HOCH_2ONO$, $CH_2O + HNO_2$, and CH_2O + HONO, respectively, are exothermic. (4) Shields et al. proposed that the $CH_2O + NO_2$ reaction occurred by a simple abstraction mechanism, leading to products $CH_2O + HNO_2$ and CH_2O + HONO. Yet, on the basis of our present calculations, we think this reaction proceeds through a complicated multistep process of association, isomerization, and dissociation as described by paths 1−4. (5) In Shields et al.' studies, the PM3 calculations predict that formation of CH_2O and HNO_2 is much more likely than the formation of CH_2O and HONO from the reaction of CH_2OH radical with NO_2. Although our results show that product $\mathbf{P_1}$ (CH_2O + *trans*-HONO) (via path 1) is the most favorable product, products $\mathbf{P_3}$ ($CH_2O + HNO_2$) (via path 3) and $\mathbf{P_4}$ (CH_2O + *cis*-HONO) (via path 4) are much less competitive products with a comparable yield. Furthermore, we also find another new possible product $\mathbf{P_2}$ (HOCHO + HNO) (via path 2). But it cannot compete with $\mathbf{P_1}$ (CH_2O + *trans*-HONO) and may have the same competition with $\mathbf{P_3}$ ($CH_2O + HNO_2$) and $\mathbf{P_4}$ (CH_2O + *cis*-HONO). (6) As can be seen from Table 1, our predicted heats of formation ($\Delta H_f^\circ{}_{298}$) of −3.5 and +9.4 kcal/mol for reactants CH_2OH and NO_2 and reaction enthalpy of −49.2 kcal/mol for product CH_2O + *trans*-HONO at the G3//B3LYP level are closer to the experimental values[35,37] of −3.1, +7.91, and −49.8, respectively, than the previous theoretical values[38] of −26.5, −15.0, and −30.4 kcal/mol, respectively, at the AM1 level and −23.5, −1.0, and −24.5 kcal/mol, respectively, at the PM3 level. The above theoretical results may provide useful information for further investigation on the title reaction.

3.4. Comparison with the $CH_3 + NO_2$ and $CH_3O + NO_2$ Reactions. It is very useful to compare the PES feature of the reaction $CH_2OH + NO_2$ with that of the analogous one $CH_3 + NO_2$. Recently, we performed a detailed theoretical investigation on the $CH_3 + NO_2$ reaction.[27] The possible reaction pathways are summarized as

Path 9: $\mathbf{R} \rightarrow \mathbf{a}$ (CH_3NO_2) $\rightarrow \mathbf{b}$ (CH_3ONO) $\rightarrow$ $\mathbf{P_1}$ (CH_3O + NO)

Path 10: $\mathbf{R} \rightarrow \mathbf{a}$ (CH_3NO_2) $\rightarrow \mathbf{b_1} \rightarrow \mathbf{P_2}$ (CH_2O + HNO)

Path 11: $\mathbf{R} \rightarrow \mathbf{a}$ (CH_3NO_2) $\rightarrow \mathbf{b_1}$ (*trans*-CH_3ONO) $\rightarrow$ $\mathbf{b_2}$ (*cis*-CH_3ONO) $\rightarrow \mathbf{P_3}$ (CH_2O + HON)

For distinction purposes, the calculated pathways for the CH_3 + NO_2 reaction are shown in italics. We found that $\mathbf{P_1}$ (CH_3O + NO) and $\mathbf{P_2}$ (CH_2O + HNO) are the most favorable products with comparable yields, whereas $\mathbf{P_3}$ (CH_2O + HON) is the least competitive product.

By comparing the theoretical results, we find that both reactions involve the same initial association way, that is, carbon-to-nitrogen association process $CH_2X + NO_2 \rightarrow XCH_2$-$NO_2$ (X = H, OH) with no barrier. The two reactions may proceed rapidly due to all of the transition states and isomers in the feasible channels lying below the reactants **R**. This is confirmed by experiments.[25,26,39] However, because the OH radical with higher electronegativity strongly attracts a nonbonded single election located at the C atom, the electron density on the carbon atom is reduced, which leads to a decreasing of the reactivity of C atom of CH_2OH attack on N atom of NO_2. Thus, theoretically, the trend of reaction rate constant is $k(CH_3) > k(CH_2OH)$, which is in line with the experimental results in quality. The experimental rate constants (298 K) of CH_2X with NO_2 are $(2.5 \pm 0.5) \times 10^{-11}$ cm^3 molecule^{-1} s^{-1} for X = H[39] and $(2.3 \pm 0.4) \times 10^{-11}$ and $(8.3 \pm 4.1) \times 10^{-12}$ cm^3 molecule^{-1} s^{-1} for X = OH,[25,26] respectively. The decrease of CH_2OH reactivity also leads to the mechanism discrepancy as well as to the different product distribution between the two reactions. First, for $CH_3 + NO_2$ reaction, the initial adduct CH_3-NO_2 can isomerize to *trans*-CH_3ONO, which can be easily converted to *cis*-CH_3ONO, followed by the O1−N single bond rupture to one major product CH_3O + NO, whereas for the $CH_2OH + NO_2$ reaction, the initial formed isomer $HOCH_2NO_2$ may take the C−N bond rupture along with a concert H-shift directly to give species CH_2O + *trans*-HONO as the most favorable product. Second, for $CH_3 + NO_2$ reaction, the other major product CH_2O + HNO formed via a 1,3-H-shift associated with the N−O bond rupture of *trans*-CH_3ONO may have comparable yields with product CH_3O + NO. However, for the $CH_2OH + NO_2$ reaction, the similar product HOCHO + HNO, which can be obtained through the isomerization of isomer $HOCH_2NO_2$ to *trans*-$HOCH_2ONO$ followed by a concert H-shift along with the O2−N bond cleavage, is kinetically much less competitive than the major product CH_2O + *trans*-HONO. Third, for the $CH_3 + NO_2$ reaction, the pathway of the O1−N bond cleavage associated with a concerted H-shift from *cis*-CH_3ONO to product CH_2O + HON can be located as the third feasible channel, whereas, for the $CH_2OH + NO_2$ reaction, isomer *cis*-$HOCH_2ONO$ may undergo a 1,4-H-shift from the O1 atom to the N atom or a 1,5-H-shift from the O1 atom to the O3 atom accompanied by C−O2 bond fission to form the less favorable product $CH_2O + HNO_2$ or CH_2O + *cis*-HONO.

On the other hand, the reaction of CH_3O with NO_2, which is more important and interesting for atmospheric chemists, has already been the subject of experimental and theoretical investigations.[40−48] Very recently, Pan et al.[48] reported the detailed mechanistic study on the radical−molecule reaction $CH_3O + NO_2$. It is necessary to make a comparison of the mechanisms between the two reactions of CH_3O and CH_2OH with NO_2. First, it is readily found that the attack of CH_3O and CH_2OH radicals on NO_2 molecule both focus on the N-site. Second, the initial association for these two reactions are both a barrierless addition process to form respective adducts $HOCH_2$-NO_2 and CH_3ONO_2. Third, for the $CH_2OH + NO_2$ reaction, the initial adduct $HOCH_2NO_2$ can further dissociate to product CH_2O + *trans*-HONO as the most competitive product. However, for the $CH_3O + NO_2$ reaction, the dissociation process from the initial adduct CH_3ONO_2 to product CH_2O + *trans*-HONO is kinetically almost inhibited because the dissociation transition state linking CH_3ONO_2 to CH_2O + *trans*-HONO lies much higher than the reactants in energy. As a result, the adduct CH_3ONO_2 is the dominant product for the reaction CH_3O with NO_2. Fourth, for the $CH_3O + NO_2$ reaction, the other two products CH_2O + *cis*-HONO and $CH_2O + HNO_2$ are kinetically unfavorable due to the significantly high barriers, whereas for the $CH_2OH + NO_2$ reaction, the pathways leading to the same two products are kinetically feasible at normal temperatures.

At the same time, both of the products are much less competitive than major product CH_2O + *trans*-HONO. Furthermore, a new product HOCHO + HNO is located for the reaction CH_2OH with NO_2 and may have an abundance similar to that of products CH_2O + *cis*-HONO and CH_2O + HNO_2. Fifth, instead of a simple abstraction mechanism, both reactions proceed through the complicated processes of association and dissociation. Last, the two reactions are expected to be fast because the transition state and isomer in the most feasible pathway lie below the reactants **R**, which is confirmed by experiments.[43,44] The theoretical results presented here are expected to provide a useful basis for further investigation on other analogous alkoxy reactions and to be helpful for understanding the NO_x-combustion chemistry.

4. Conclusions

A detailed potential energy surface of the CH_2OH + NO_2 reaction system has been characterized at the B3LYP and G3 (single-point) levels. The main results can be summarized as follows: (1) This reaction proceeds mostly through singlet pathways and less go through triplet pathways. (2) It is most likely initiated by the carbon-to-nitrogen approach to form adduct **1** ($HOCH_2NO_2$) with no barrier. Subsequently, isomer **1** can directly dissociate to $\mathbf{P_1}$ (CH_2O + *trans*-HONO) as the most feasible product. Much less competitively, isomer **1** can undergo successive isomerization and fission processes to products $\mathbf{P_2}$ (HOCHO + HNO), $\mathbf{P_3}$ (CH_2O + HNO_2), and $\mathbf{P_4}$ (CH_2O + *cis*-HONO). (3) Formation of products $\mathbf{P_7}$ (*trans*-OCHNO + H_2O), $\mathbf{P_8}$ (*cis*-OCHNO + H_2O), $\mathbf{P_9}$ (*trans*-HOCNO + H_2O), and $\mathbf{P_{10}}$ (HONCO + H_2O) may become feasible at high temperatures. The other reaction pathways are surely energetically inaccessible due to significantly high barriers. (3) Because the isomer and transition state involved in the most favorable pathway (path 1) are all lower than the reactants **R** in energy, the CH_2OH + NO_2 reaction is expected to be fast, as is confirmed by experiment. So the CH_2OH + NO_2 reaction may be of significance in atmospheric and combustion chemistry. (4) Further comparisons are made on the PES of the CH_2OH + NO_2 reaction with that of CH_3 + NO_2 and CH_3O + NO_2 reactions. For the CH_2X + NO_2 (X = H, OH) reactions, the total rate constants increase from X = OH to X = H with the decreased electronegativity.

This study may provide useful information on the reaction mechanism and assist in further laboratory identification of the products.

Acknowledgment. This work is supported by the National Natural Science Foundation of China (20333050, 20303007), the Doctor Foundation by the Ministry of Education, the Foundation for University Key Teacher by the Ministry of Education, the Key Subject of Science and Technology by the Ministry of Education of China, and the Innovation Foundation by Jilin University.

Supporting Information Available: Harmonic vibrational frequencies and B3LYP/6-311G(d,p) optimized geometries. This material is available free of charge via the Internet at http://pubs.acs.org.

References and Notes

(1) Tsang, W.; Hampson, R. F. *J. Phys. Chem. Ref. Data* **1986**, *15*, 1087.

(2) Warnatz, J. In *Combustion Chemistry*; Gardiner, W. C. Jr., Ed.; Springer-Verlag: New York, 1984.

(3) Westbrwk, C. K.; Dryer, F. L. *Combust. Sci. Technol.* **1979**, *20*, 125.

(4) Niki, H.; Maker, P. D.; Savage, C. M.; Breitenbach, L. P. *J. Phys. Chem.* **1978**, *82*, 135.

(5) Atkinson, R. *Chem. Rev.* **1985**, *85*, 69.

(6) Wendt, H. R.; Hunziker, H. E. *J. Chem. Phys.* **1979**, *71*, 5202.

(7) Gutman, D.; Sanders, N.; Butler, J. E. *J. Phys. Chem.* **1982**, *86*, 66.

(8) Morabito, P.; Heiklen, J. *J. Phys. Chem.* **1985**, *89*, 2914 and references therein.

(9) Radford, H. E. *Chem. Phys. Lett.* **1980**, *71*, 195.

(10) Wang, W. C.; Suto, M.; Lee, L. C. *J. Phys. Chem.* **1984**, *81*, 3122.

(11) Grotheer, H. H.; Riekert, G.; Meier, U.; Just, T. *Ber. Bunsen-Ges. Phys. Chem.* **1985**, *89*, 187.

(12) Dobe, S.; Temps, F.; Bohland, T.; Wagner, H. *Gg. Z. Nuturforsch.* **1985**. *40a*, 1289.

(13) Payne, W. A.; Brunning, J.; Mitchell, M. B.; Stief, L. J. *Int. J. Chem. Kinet.* **1988**, *20*, 63.

(14) Baren, R. E.; Erickson, M. A.; Hershberger, J. F. *Int. J. Chem. Kinet.* **2002**, *34*, 12.

(15) Rim, K. T.; Hershberger, J. F. *J. Phys. Chem. A* **1998**, *102*, 4592.

(16) (a) Lanier, W. S.; Mulholland, J. A.; Beard, J. T. *Symp. (Int.) Combust. [Proc.]* **1988**, *21*, 1171. (b) Chen, S. L.; McCarthy. J. M.; Clark, W. D.; Heap, M. P.; Seeker, W. R.; Pershing, D. W. *Symp. (Int.) Combust. [Proc.]* **1988**, *21*, 1159.

(17) Myerson, A. L. In *15th Symposium (International) on Combustion*; The combustion Institute: Pittsburgh, PA, 1975; p 1085.

(18) Song, Y. H.; Blair, D. W.; Siminski, V. J.; Bartok, W. In *18th Symposium (International) on Combustion*; The Combustion Institute: Pittsburgh, PA, 1981, p 53.

(19) Chen, S. L.; McCarthy, J. M.; Clark, W. D.; Heap, M. P.; Seeker, W. R.; Pershing, D. W. In *21st Symposium (International) on Combustion*; The Combustion Institute: Pittsburgh, PA, 1986; p 1159.

(20) Faravelli, T.; Frassoldati, A.; Ranzi, E. *Combust. Flame* **2003**, *132*, 188.

(21) Wagener, R.; Wagner, H. *Gg. Z. Phys. Chem.* **1992**, *175*, 9.

(22) Hancock, G.; Ketley, G. W. *J. Chem. Soc., Faraday Trans.* **1982**, *78*, 1283.

(23) Baren, R. E.; Erickson, M. A.; Hershberger, J. F. *Int. J. Chem. Kinet.* **2002**, *34*, 12.

(24) Cookson, J. L.; Hancock, G.; Mckendrick, K. G. *Ber. Bunsen-Ges. Phys. Chem.* **1985**, *89*, 335.

(25) Nesbitt, F. L.; Payne, W. A.; Stief, L. J. *J. Phys. Chem.* **1989**, *93*, 5158.

(26) Pagsberg, P.; Munk, J.; Anastasi, C.; Simpson, V. J. *J. Phys. Chem.* **1989**, *93*, 5162.

(27) Zhang, J. X.; Liu, J. Y.; Li, Z. S.; Sun, C. C. *J. Comput. Chem.* **2005**, *26*, 807.

(28) Frisch, M. J.; Trucks, G. W.; Schlegel, H. B.; Scuseria, G. E.; Robb, M. A.; Cheeseman, J. R.; Zakrzewski, V. G.; Montgomery, J. A., Jr.; Stratmann, R. E.; Burant, J. C.; Dapprich, S.; Millam, J. M.; Daniels, A. D.; Kudin, K. N.; Strain, M. C.; Farkas, O.; Tomasi, J.; Barone, V.; Cossi, M.; Cammi, R.; Mennucci, B.; Pomelli, C.; Adamo, C.; Clifford, S.; Ochterski, J.; Petersson, G. A.; Ayala, P. Y.; Cui, Q.; Morokuma, K.; Malick, D. K.; Rabuck, A. D.; Raghavachari, K.; Foresman, J. B.; Cioslowski, J.; Ortiz, J. V.; Stefanov, B. B.; Liu, G.; Liashenko, A.; Piskorz, P.; Komaromi, I.; Gomperts, R.; Martin, R. L.; Fox, D. J.; Keith, T.; Al-Laham, M. A.; Peng, C. Y.; Nanayakkara, A.; Gonzalez, C.; Challacombe, M.; Gill, P. M. W.; Johnson, B. G.; Chen, W.; Wong, M. W.; Andres, J. L.; Head-Gordon, M.; Replogle, E. S.; Pople, J. A. *Gaussian 98*, revision A.9; Gaussian, Inc.: Pittsburgh, PA, 1998.

(29) Becke, A. D. *J. Chem. Phys.* **1993**, *98*, 5648.

(30) McLean, A. D.; Chandler, G. S. *J. Chem. Phys.* **1980**, *72*, 5639.

(31) Krishnan, R.; Binkley, J. S.; Seeger, R.; Pople, J. A. *J. Chem. Phys.* **1980**, *72*, 650.

(32) Frisch, M. J.; Pople, J. A.; Binkley, J. S. Self-Consistent Molecular Orbital Methods 25: Supplementary Functions for Gaussian Basis Sets. *J. Chem. Phys.* **1984**, *80*, 3265.

(33) Curtiss, L. A.; Raghavachari, K.; Redforn, P. C.; Rassolov, V.; Pople, J. A. *J. Chem. Phys.* **1998**, *109*, 7764.

(34) Kuchitsu, K. *Structure of Free Polyatomic Molecules Basic Data*; Springer-Verlag: Berlin, 1998.

(35) Lide, D. R. in *CRC Handbook of Chemistry and Physics*, 80th ed.; CRC Press: Boca Raton, FL, 1999.

(36) The harmonic vibrational frequencies of important species at the B3LYP/6-311G(d,p) level are given in Table S1. The B3LYP/6-311G(d,p) optimized geometries of unfavorable species are presented in Figure S1.

(37) In *NIST Chemistry WebBook*, NIST Standard Reference database Number 69, March 2003 Release. Vibrational frequency data compiled by M. E. Jacox (http://www.webbook.nist.gov).

(38) Kalkanis, G. H.; Shields, G. C. *J. Phys. Chem. A* **1991**, *95*, 5085.

(39) Yamada, F.; Slagle, I. R.; Gutman, D. *Chem. Phys. Lett.* **1981**, *83*, 409.

(40) McCaulley, J. A.; Anderson, S. M.; Jeffries, J. B. *Chem. Phys. Lett.* **1995**, *115*, 180.
(41) Frost, M. J.; Smith, I. W. M. *J. Chem. Soc., Faraday Trans.* **1990**, *86*, 1751.
(42) Biggs, P.; Canosa-Mas, C. E.; Fracheboud, J. M. *J. Chem. Soc., Faraday Trans.* **1993**, *89*, 4163.
(43) Martinez, E.; Albaladejo, J.; Jimenez, E. *Chem. Phys. Lett.* **2000**, *329*, 191.
(44) Wollenhaupt, M.; Crowley, J. N. *J. Phys. Chem. A* **2000**, *104*, 6429.
(45) Lohr, L. L.; Baker, J. R.; Shroll, R. M. *J. Phys. Chem. A* **2003**, *107*, 7429.
(46) Baker, J. R.; Lohr, L. L.; Shroll, R. M.; Reading, S. *J. Phys. Chem. A* **2003**, *107*, 7434.
(47) Zhang, D.; Zhang, R.; Park, J.; North, S. W.; *J. Am. Chem. Soc.* **2002**, *124*, 9600.
(48) Pan, X. M.; Fu, Z.; Li, Z. S.; Sun, C. C.; Sun, H.; Su, Z. M.; Wang, R. S. *Chem. Phys. Lett.* **2005**, *409*, 98.